Champneys, A. R., & Thompson, J. M. T. (1994). A multiplicity of localised buckling modes for twisted rod equations.

A Multiplicity of Localized Buckling Modes for Twisted Rod Equations

A.R. Champneys & J.M.T. Thompson

Department of Engineering Mathematics
Queens Building, University of Bristol
Bristol BS8 1TR, U.K.

Centre for Nonlinear Dynamics
Civil Engineering Building
University College
London WC1E 6BT, U.K.

To Appear in Proc. Roy. Soc. A 1996

Abstract

The Kirchhoff-Love equations governing the spatial equilibria of long thin elastic rods subject to end tension and moment are reviewed and used to examine the existence of localized buckling solutions. The effects of shear and axial extension are not considered, but the model does additionally allow for nonlinear constitutive laws. Under the assumption of infinite length, the dynamical phase space analogy allows one to use techniques from dynamical systems theory to characterise many possible equilibrium paths. Localizing solutions correspond to *homoclinic orbits* of the dynamical system. Under non-dimensionalisation the twisted rod equations are shown to depend on a single load parameter, and the bifurcation behaviour of localizing solutions of this problem is investigated using analytical and numerical techniques.

First, in the case of a rod with equal principal bending stiffnesses, where the equilibrium equations are completely integrable, a known one-parameter family of localizing solutions is computed for a variety of subcritical loads. Load-deflection diagrams are computed for this family and certain materially non-linear constitutive laws are shown to make little difference to the qualitative picture.

The breaking of the geometrical circular symmetry destroys complete integrability and, in particular, breaks the non-transverse intersection of the stable and unstable manifolds of the trivial steady state. The resulting transverse intersection, which is already known to lead to spatial chaos, is explicitly demonstrated to imply multitude of localized buckling modes. A sample of primary and *multi-modal* solutions are computed numerically, aided by the reversibility of the differential equations.

Finally, parallels are drawn with the conceptually simpler problem of a strut resting on a (non-linear) elastic foundation, for which much more information is known about the global behaviour of localized buckling modes.

1 Introduction

In an earlier paper (Thompson & Champneys 1995), we considered experimental aspects of the buckling of long, thin elastic rods subject to applied end loads, and used energy methods to compare the characteristics of two buckling modes. In the present paper we extend this analysis using a mathematical formulation of equilibrium equations for the idealisation of an infinitely long rod. We concentrate almost exclusively on localizing solutions, and use dynamical systems techniques to extend our focus to a potentially infinite number of buckling modes.

The study of the three-dimensional spatial equilibria of thin elastic rods dates at least as far back as Kirchhoff (1859). He showed that there is a direct analogy between the equations describing equilibrium positions of an infinite rod and the dynamics of a spinning top (see also (Mielke & Holmes 1988, Davies & Moon 1993)). This was the first example of what is now known as the dynamic phase space analogy. Here, the arclength s along the central axis of the rod plays the rôle of time. If one considers infinite rods with all constraints applied at one end, then the analogy with an initial-value problem is complete. Care has to be taken, however, to treat the appropriate two-point boundary-value problem when considering rods of finite length or localizing solutions of rods that are assumed to be infinite. Love (1927) noticed that an ordinarily straight rod whose principal bending stiffnesses are equal can be bent via end forces and moments into the form of a helical wave, corresponding to a periodic orbit of the spinning top. The key to this analysis was the recognition that the Kirchhoff-Love equations are *completely integrable*. More recently, Coyne (1990) showed that the same integrability implies the existence of a localizing solution, corresponding to a homoclinic orbit of the dynamical system. An analysis of the comparative bifurcational behaviour of these two classical buckling modes is given in (Thompson & Champneys 1995).

The modern theory of elastic rod buckling began with the work of Antman and co-workers (see Antman & Kenney (1981) and references therein). They consider a more general formulation that allows additionally for shear deformations and axial extensibility of the material of the rod, as well as for arbitrary constitutive laws ("stress-strain" relations). Mielke & Holmes (1988) exploited the Hamiltonian structure of such a formulation to show that, for the more general model of Antman and Kenney, circular symmetry in the cross-section of the rod always implies complete integrability. In the present setting, this implies the existence of a continuum (a smooth manifold) of localizing solutions. Some other symmetry properties of rods with polygonal cross-sections are taken up in Buzano, Geymonat & Poston (1985) and Pierce (1991), but do not concern us here.

The main result of Mielke & Holmes (1988) is to show that abandoning circular symmetry (e.g. considering a tape, rather than a tube) in general destroys complete integrability and hence breaks the non-transverse intersection of stable and unstable manifolds along the manifold of localizing solutions. Melnikov's method is then used to argue the existence of spatially chaotic solutions nearby. Davies & Moon (1993) used a physically unrealistic model of a twisted rod subject to no external forces, but with a periodic non-uniformity along its length, to compute beautiful 3D pictures of some spatially chaotic equilibria. It was not stated by Mielke and Holmes, but is argued in §3 below, that the spatial chaos also implies the existence of infinitely many *multi-modal* homoclinic solutions (see, for example, Fig. 12 below). These solutions represent localized buckling modes which, as shown in (Thompson & Champneys 1995), are the physically prefered modes for long rods.

Finally, we mention related work on the *dynamics* of rods, especially on solitary waves (e.g. Coleman, Dill, Lembo, Lu & Tobias (1993), Maddocks & Dichman (1994), Dichmann, Maddocks & Pego (1993)) which with zero wavespeed represent localized static modes.

The aim of the present paper is to present for the first time a coherent account of the multiplicity of localized buckling modes arising in the Kirchoff-Love Theory. We present an elementary derivation of the equilibrium equations of an infinite rod subject to applied end moment and tension. A new non-dimensionalisation of this model shows that the equations are characterised by only two dimensionless parameters, representing the loading and the cross-sectional geometry. We then go on to explore by linearisation, generic dynamical systems arguments and numerical computations, the existence of localized buckling modes in various regions of parameter space, with both linear and nonlinear constitutive laws. In the simplest case (when the geometric parameter is zero and with linear constitutive laws) we recover known results, thus justifying our numerical methods. In all other cases our numerical results are completely new.

Our results show remarkable similarities with those known for a model of an infinite strut resting on a nonlinearly elastic foundation [1] for which a lot of information on the global structure of multi-modal homoclinic solutions is now known (Thompson & Virgin 1988, Hunt, Bolt & Thompson 1989, Hunt & Wadee 1991, Amick & Toland 1992, Buffoni & Toland 1994, Champneys & Toland 1993, Buffoni, Champneys & Toland 1994). In contrast, far less is known about spatial localisation in twisted rods. Thus, the strut model gives indications of further global results we may expect to hold for the rod.

The rest of the paper is outlined as follows. In §2 we consider the mathematical formulation of the twisted rod problem. §3 then concerns linearisation, existence theory, normal-form and symmetry arguments applied to this system. §4 contains numerical computations of localizing solutions. The results in §3 and §4 are presented for three different types of rod: for circular rods with either linear or certain non-linear constitutive laws, and for non-circular rods with linear constitutive laws. Finally, in §5 we draw comparisons with the simpler elastic strut model and make suggestions for future work.

2 Twisted rod equations

Our formulation of equilibrium equations for a twisted rod follows the seminal treatment in Love (1927) using the notation of Davies & Moon (1993). We additionally allow for more general constitutive equations (Antman & Kenney 1981). Note that, as in Love, we do not consider the effects of shear deformations or axial extensions of the rod, although a consistent formulation requires their inclusion (see Antman & Kenney (1981), Mielke & Holmes (1988) and §2.1 below). We also ignore gravity or any other external forces applied other than at the ends of the rod. While we do not expect these extra effects to qualitatively alter our results, we shall leave their investigation to future work.

[1] which equation also describes in a mathematically rigorous sense, solitary water waves in the presence of surface tension(Champneys & Toland 1993, Buffoni, Groves & Toland 1995)

2.1 Forces and Moments

Consider an infinitely long, thin rod which, when subject to no external forces, is straight and prismatic with a uniform cross-section. We suppose that the rod is subject to loads in the form of a twisting moment M about the centerline and tension T applied at its ends, see Thompson & Champneys (1995, Fig. 1). In order to describe the spatial configuration of the rod, choose an origin for an arclength co-ordinate s and then define $\boldsymbol{r}(s)$ to be the position vector of the centre line. Define a right-handed set of co-ordinates (x, y, z) such that z points along the centre line of the rod at $s = 0$, i.e. $\boldsymbol{r}'(0) = (0, 0, 1)$, and any cross-section of the unstrained rod that is orthogonal to the centre line lies parallel to the (x, y)-plane. In addition, define a rod-centred moving orthonormal co-ordinate system $(\boldsymbol{e}_1(s), \boldsymbol{e}_2(s), \boldsymbol{e}_3(s))$ to be such that $\boldsymbol{e}_3(s) = \boldsymbol{r}'(s)$ is everywhere tangent to the central axis of the rod, and $\boldsymbol{e}_{1,2}(s)$, which together define the cross-section at s, are fixed to the material of the rod that, when totally unstrained, was aligned with the x and y axes respectively.

As dependent variables for the dynamical analogy, we will take the contact forces $(F_1(s), F_2(s), F_3(s))$ and couples $(G_1(s), G_2(s), G_3(s))$, defined such that the resultant force $\mathcal{F}(\hat{s})$ and moment $\mathcal{G}(\hat{s})$ exerted by the material parametrised by $s < \hat{s}$ on that with $s > \hat{s}$ are given by

$$\mathcal{F}(\hat{s}) = F_1(\hat{s})\boldsymbol{e_1} + F_2(\hat{s})\boldsymbol{e}_2 + F_3(\hat{s})\boldsymbol{e_3}, \quad \mathcal{G}(\hat{s}) = G_1(\hat{s})\boldsymbol{e}_1 + G_2(\hat{s})\boldsymbol{e}_2 + G_3(\hat{s})\boldsymbol{e}_3. \tag{2.1}$$

Here $F_{1,2}$ are shear forces, F_3 is tension, $G_{1,2}$ are bending moments about the axes $\boldsymbol{e}_{1,2}$ and G_3 is the twisting moment about the centre line.

Now, let the strain of the rod be given by $\Omega(s) = \kappa_1(s)\boldsymbol{e}_1 + \kappa_2(s)\boldsymbol{e}_2 + \tau(s)\boldsymbol{e}_3$, where τ is the torsion or rate of twist about the centerline (see Thompson & Champneys (1995, §4.1a)), and $\kappa_{1,2}$ are the principal curvatures about $\boldsymbol{e}_{1,2}$ respectively. Then, balancing forces and moments at arclength s leads to the equations (cf. eqs. (10),(11) in art. 254 of Love (1927))

$$\mathcal{F}' = \mathcal{F} \times \Omega \tag{2.2}$$

$$\mathcal{G}' = \mathcal{G} \times \Omega - \boldsymbol{e}_3 \times \mathcal{F}, \tag{2.3}$$

where all vectors are expressed with respect to the moving basis $(\mathbf{e}_1, \boldsymbol{e}_2, \boldsymbol{e}_3)$. Note that to take shear and axial-extensibility into account requires the definition of an additional 'strain' vector $\boldsymbol{v}$ whose first two components are shears in the directions $\boldsymbol{e}_{1,2}$, and whose third component is axial extension. The inclusion of these effects into the model leads only to the addition of a term $\boldsymbol{v} \times \mathcal{F}$ to the right-hand side of (2.3) (cf. eq. (2.7) of Mielke & Holmes (1988)) and a re-definition of the derivative since the unstrained arclength s no longer measures the length of the centre line of an axially extended rod.

2.2 Constitutive relations

It remains to specify the strains Ω in terms of the stresses $\mathcal{F}$ and $\mathcal{G}$. The simplest assumption (cf. art. 255 of Love (1927)) is to take linear constitutive laws

$$\kappa_1 = G_1/A, \quad \kappa_2 = G_2/B, \quad \tau = G_3/C,$$

where A and B are the principal bending stiffnesses (about the $\boldsymbol{e}_1$ and $\boldsymbol{e}_2$ axes respectively) and C the torsional stiffness of the rod. The assumption of a circular cross-section implies $A = B$

(B is the constant appearing in the linear eigenvalue condition in Thompson & Champneys (1995, eq. (2.1))).

Since we shall be interested in large-amplitude deflections it is realistic to include the effect of nonlinearities in the constitutive relations. Following Antman & Kenney (1981), under the assumption of transverse isotropy (i.e. the material properties obey circular symmetry about the centre line), and keeping only the lowest-order nonlinear terms, the most general constitutive relations take the form

$$\kappa_1 = G_1\mu/A, \quad \kappa_2 = G_2\mu/B, \quad \tau = G_3\eta/C, \tag{2.4}$$

where

$$\mu(\mathcal{F},\mathcal{G}) = 1 + \alpha_1 G_1^2 + \alpha_2 G_1F_1 + \alpha_3 F_1^2 + \alpha_4 G_2^2 + \alpha_5 G_2F_2 + \alpha_6 F_2^2 + \alpha_7 G_3^2 + \alpha_8 F_3^2, \tag{2.5}$$

$$\eta(\mathcal{F},\mathcal{G}) = 1 + \beta_1 G_1^2 + \beta_2 G_1F_1 + \beta_3 F_1^2 + \beta_4 G_2^2 + \beta_5 G_2F_2 + \beta_6 F_2^2 + \beta_7 G_3^2 + \beta_8 F_3^2, \tag{2.6}$$

for constants α_i, β_i, $i = 1, \ldots 8$, subject to certain constraints (see Antman & Kenney (1981, Eqs. (2.20),(2.21))).

Given the relations (2.4)–(2.6), the equations (2.2), (2.3) define a dynamical system in a six-dimensional phase space with co-ordinates $(G_1, G_2, G_3, F_1, F_2, F_3)$.

2.3 Transformation to physical space co-ordinates

Under the given assumptions, a solution to (2.2), (2.3) completely specifies an equilibrium configuration of the rod. However, in order to interpret such a solution in terms of the fixed co-ordinates (x, y, z), one has also to solve the so-called Frenet-Seret equations of differential geometry (cf. eqs. (5) of art. 253 in Love (1927))

$$\boldsymbol{e}_i' = \Omega \times \boldsymbol{e}_i, \quad i = 1, 2, 3, \tag{2.7}$$

as well as the obvious defining equations for the centre line

$$\boldsymbol{r}' = \boldsymbol{e}_3. \tag{2.8}$$

Taking as dependent variables the x, y and z components of each of the vectors $\boldsymbol{e}_i$, $i = 1, \ldots, 3$, and $\boldsymbol{r}$, the equations (2.7) and (2.8) form a coupled system of twelve ODEs that should be solved in tandem with (2.2) and (2.3), but contain no new dynamical information. Instead they should be considered as "slaves" which post-process the data obtained from the dynamical system. (Here we are thinking of an initial-value problem; when solving a boundary-value problem one may have to consider (2.2), (2.3), (2.7) and (2.8) as a completely coupled system, depending on how exactly the boundary conditions are imposed, cf. Mahadevan & Keller (1993, 1995)).

2.4 Non-dimensionalisation

First note that the applied twisting moment M and tension T do not enter equations (2.2) and (2.3). However, if we make the change of variables

$$\tilde{F}_3 = F_3 - T, \quad \tilde{G}_3 = G_3 - M, \tag{2.9}$$

then, under a given (pre-fixed or controlled) load (M, T), the trivial equilibrium position of the rod is $(F_1, F_2, \tilde{F}_3, G_1, G_2, \tilde{G}_3) = (0, 0, 0, 0, 0, 0)$, the origin of the new phase space.

Second, note that we can non-dimensionalise by defining new variables

$$\begin{aligned} x_1 &= F_1/T, \quad x_2 = F_2/T, \quad x_3 = \tilde{F}_3/T \\ x_4 &= G_1/M, \quad x_5 = G_2/M, \quad x_6 = \tilde{G}_3/M, \end{aligned} \tag{2.10}$$

re-scaling the axial length via

$$t = \frac{M}{B}\, s, \tag{2.11}$$

and introducing the dimensionless parameters

$$m = M/\sqrt{BT}, \quad \rho = (B/A) - 1, \quad \nu = (B/C) - 1. \tag{2.12}$$

In the dimensionless variables the equations (2.2) and (2.3) become

$$\left.\begin{aligned} \dot{x}_1 &= (1+\nu)\,\tilde{\eta}(\boldsymbol{x})\,x_2\,(1+x_6) - \tilde{\mu}(\boldsymbol{x})\,(1+x_3)\,x_5 \\ \dot{x}_2 &= (1+\rho)\,\tilde{\mu}(\boldsymbol{x})\,(1+x_3)\,x_4 - (1+\nu)\,\tilde{\eta}(\boldsymbol{x})\,x_1\,(1+x_6) \\ \dot{x}_3 &= \tilde{\mu}(\boldsymbol{x})\,x_1\,x_5 - (1+\rho)\,\tilde{\mu}(\boldsymbol{x})\,x_2\,x_4 \\ \dot{x}_4 &= [\,(1+\nu)\,\tilde{\eta}(\boldsymbol{x}) - \tilde{\mu}(\boldsymbol{x})\,]\,x_5\,(1+x_6) + x_2/m^2 \\ \dot{x}_5 &= [\,(1+\rho)\,\tilde{\mu}(\boldsymbol{x}) - (1+\nu)\,\tilde{\eta}(\boldsymbol{x})\,]\,x_4\,(1+x_6) - x_1/m^2 \\ \dot{x}_6 &= -\rho\tilde{\mu}(\boldsymbol{x})\,x_4\,x_5 \end{aligned}\right\} \tag{2.13}$$

where '$\cdot$' denotes differentiation with respect to the new arclength t and $\tilde{\mu}(\boldsymbol{x}), \tilde{\eta}(\boldsymbol{x})$ are non-dimensionalised versions of $\mu(\mathcal{F}, \mathcal{G}), \eta(\mathcal{F}, \mathcal{G})$:

$$\tilde{\mu}(\boldsymbol{x}) = 1 + a_1 {x_4}^2 + a_2 x_4 x_1 + a_3 {x_1}^2 + a_4 {x_5}^2 + a_5 x_5 x_2 + a_6 x_2^2 + a_7 (1+x_6)^2 + a_8 (1+x_3)^2, \tag{2.14}$$

$$\tilde{\eta}(\boldsymbol{x}) = 1 + b_1 x_4^2 + b_2 x_4 x_1 + b_3 x_1^2 + b_4 x_5^2 + b_5 x_5 x_2 + b_6 x_2^2 + b_7 (1+x_6)^2 + b_8 (1+x_3)^2, \tag{2.15}$$

for dimensionless constants a_i, b_i, $i = 1, \ldots, 8$, related to the α_i, β_i.

The dimensionless versions of (2.7) and (2.8) are

$$\dot{\boldsymbol{e}}_i = \tilde{\Omega} \times \boldsymbol{e}_i, \quad i = 1, 2, 3, \tag{2.16}$$

$$\dot{\tilde{\boldsymbol{r}}} = \boldsymbol{e}_3, \tag{2.17}$$

where

$$\tilde{\Omega} = (1+\rho)\tilde{\mu} x_4\, \boldsymbol{e}_1 + \tilde{\mu} x_5\, \boldsymbol{e}_2 + (1+\nu)\tilde{\eta}(1+x_6)\, \boldsymbol{e}_3 \quad \text{and} \quad \tilde{\boldsymbol{r}} = (M/B)\boldsymbol{r}.$$

2.5 Integrals of the motion

Mielke & Holmes (1988) show that, for general constitutive laws (including the case where shear and axial extensibility are included), the equations (2.2) and (2.3) represent an autonomous Hamiltonian system of three degrees of freedom (i.e. a six-dimensional phase space). The Hamiltonian function is related to the strain energy function of elasticity theory. Furthermore, in Mielke & Holmes (1988, §3) it is shown that the Hamiltonian system is degenerate, because there always exist two independent integrals of the motion corresponding to the conservation

of the magnitude of force and the component of torque about the loading axis along the axial length of the rod. That is, for any given solution of (2.13),

$$|\mathcal{F}|^2 = x_1^2 + x_2^2 + (x_3 + 1)^2 = \text{const.}, \tag{2.18}$$

$$\langle \mathcal{F}, \mathcal{G} \rangle = x_1\, x_4 + x_2\, x_5 + (1 + x_3)\,(1 + x_6) = \text{const.}, \tag{2.19}$$

for all t. Thus, the dynamics of a trajectory of (2.13) with given $|\mathcal{F}|$ and $\langle \mathcal{F}, \mathcal{G} \rangle$ may be regarded as evolving in a *four-dimensional phase space*, independent of the constants a_i, b_i, ρ and ν.

Love (1927, art. 260) considers the special case of linear constitutive laws, i.e. taking $\tilde{\eta} = \tilde{\mu} = 1$. Then, note that eliminating x_1 and x_2 in the third equation of (2.13) using the last three equations, results in a total derivative, namely that

$$H = 2x_3 + m^2 \left[(1 + \rho) x_4^2 + x_5^2 + (1 + \nu)(x_6 + 1)^2 \right] = \text{const.} \tag{2.20}$$

The function H is the Hamiltonian for this case. A similar (but algebraically more cumbersome) expression for the Hamiltonian function could be derived in the case of general $\tilde{\eta}$ and $\tilde{\mu}$. Note that (2.18), (2.19) and (2.20) do not represent three independent *isolating integrals* of (2.13) and therefore, the Hamiltonian system is not necessarily *completely integrable* in the classical sense (see for example Lichtenberg & Lieberman (1992, §1.3)).

Given the additional simplification of a rod with circular cross-section (or a rod with linear constitutive relations for which the principal bending stiffnesses are equal, e.g. a rod having square cross-section) we have that $A = B$ and hence $\rho = 0$. Note that the right-hand side of the final equation of (2.13) then becomes identically zero. Hence, we obtain the additional integral (cf. eq. (33) in art. 269 of (Love 1927))

$$x_6 = \text{const.} \tag{2.21}$$

Now (2.18), (2.19) and (2.21) *do* represent three independent isolating integrals, and hence the system is completely integrable, which specifically precludes the possibility of chaotic solutions. It is the existence of the three integrals (2.18)–(2.21) in this special case that has allowed a detailed analysis of the helix and localizing solution (Love 1927, Coyne 1990, Coleman et al. 1993, Thompson & Champneys 1995).

2.6 The three cases

In what follows we shall consider the above model in the three special cases:

1. Circular cross-section, linear constitutive relations; $\rho = 0$, $\tilde{\mu} = \tilde{\eta} = 1$.
2. Circular cross-section, simplest non-linear constitutive relations; $\rho = 0$, $\tilde{\mu} = 1$, $b_7, b_8 \neq 0$.
3. Non-circular cross-section, linear constitutive relations; $\rho \neq 0$, $\tilde{\mu} = \tilde{\eta} = 1$.

Note that, according to the theory of §2.5, Cases 1 and 2 imply complete integrability, whereas 3 does not. We remark that the nonlinear constitutive relations in Case 2 describe a softening (or hardening) in the twisting moment vs. torsional strain relation, which may well be realistic for the modeling of helically reinforced electrical and marine cables (Coyne 1990, p. 73).

3 Analytical considerations

In this section we discus some analytical results applied to (2.13) of relevance to the torsional buckling of long rods Our interest is in localizing solutions, that is solutions that satisfy the homoclinic boundary conditions

$$\boldsymbol{x} \to 0 \text{ as } t \to \pm\infty,$$

as these were shown in Thompson & Champneys (1995) to be the physically preferred buckling modes for long rods. Hence, employing the Kirchhoff dynamical analogy of the spatial configuration of rods, we regard (2.13) as a six-dimensional dynamical system on the real line, for which we are interested in only homoclinic solutions to the origin. First we consider the linearisation at the origin, which is crucial for the multiplicity results which follow.

3.1 Linearisation

Upon linearisation of (2.13) about the trivial equilibrium $\boldsymbol{x} = \mathbf{0}$, one obtains the characteristic polynomial

$$\begin{aligned} &\lambda^6 + \left[\Big(a^2 - a(Q+bN)\Big)\, R - a\,(Q+bN) + 2\,b^2N^2\right]\lambda^4 \\ &+ \left[\Big((Q^2 + b^2N^2 - 2QbN)a^2 + (Qb^2N^2 - b^3N^3)a\Big)\, R + (Qb^2N^2 - b^3N^3)a + b^4N^4\right]\lambda^2 \end{aligned} \tag{3.1}$$

where

$$b = 1 + b_7 + b_8, \quad a = 1 + a_7 + a_8, \quad N = (1+\nu), \quad R = (1+\rho) \quad \text{and} \quad Q = 1/m^2.$$

Note that there are thus always two trivial eigenvalues. The corresponding eigenvectors are aligned along the x_3 and x_6 axes, due to the existence of other equilibria with arbitrary non-zero constant values of x_3 and x_6. Moreover, the eigenspace corresponding to the other four eigenvalues is orthogonal to these axes. We now consider the behaviour of the four non-trivial eigenvalues in each of the three special cases mentioned above, and the implications for the physical stability of the trivial equilibrium position.

Case 1 Under the substitution $\rho = 0$, $\tilde{\mu} = \tilde{\eta} = 1$, the non-trivial roots of (3.1) become

$$\frac{1}{2}\left(\pm\sqrt{(4/m^2) - 1} \;\pm i\,(1+2\nu)\right) \tag{3.2}$$

From the form of these eigenvalues we note that when $m = m_c = 2$, there are a two double imaginary eigenvalues $\pm i\,(1+2)$ and that as m varies through m_c, a Hamiltonian Hopf bifurcation occurs (van der Meer 1985). As m varies, the stability of the trivial equilibrium is as depicted in Fig. 2(b) of Thompson & Champneys (1995); the origin is a saddle-focus (a complex quadruple of eigenvalues) for $0 < m < 2$, and it is a center (four imaginary eigenvalues) for $m > 2$. Recall also from that figure that a saddle-focus corresponds to the spatial stability of the trivial equilibrium and a center to its instability. Note finally, that $m_c = 2$ corresponds to the dimensionless version of the classical Timoshenko eigenvalue condition; the condition (2.1) in Thompson & Champneys (1995).

Case 2 Substituting just $\rho = 0$, into (3.1) results in the non-trivial roots

$$\frac{1}{2}\left(\pm\sqrt{(4/m^2)-1}\ \pm i(2b(1+\nu)-a)\right). \tag{3.3}$$

Putting $a = 1$ and $b = 1 + b_7 + b_8$ we get that the critical load is still $m_c = 2$ and that the stability of the trivial equilibrium is qualitatively the same as case 1, provided

$$\nu \neq \frac{1}{2b} - 1. \tag{3.4}$$

Recall Thompson & Champneys (1995, §2) that ν is Poisson's ratio in the case of linear constitutive relations, and taking $\nu \approx 1/3$ in the limit of small $b - 1$, we see that (3.4) is satisfied in this limit.

Case 3 Upon introduction of non-zero ρ into (3.1), the nice closed form expression (3.3) for the non-trivial eigenvalues disappears, even after assuming linear constitutive laws (setting $a = b = 1$). However, by setting (3.1) and its λ-derivative equal to zero, we can find an expression for m_c, the m-value at which a Hamiltonian-Hopf bifurcation occurs (more specifically this is the condition for a double eigenvalue and will also pick up other bifurcations or degeneracies in eigenvalues). Hence we obtain that m_c is given by solutions of

$$\rho^2 m_c^{-4} + \left(-16\,\nu - 16\,\nu^2 - 8\,\rho\,\nu^2 + 2\,\rho - 4 + 2\,\rho^2\nu\right) m_c^{-2} + 4\,\rho\,\nu^2 + 4\,\nu^2 + 1 + 4\,\nu + 2\,\rho\,\nu + \rho^2\nu^2 = 0. \tag{3.5}$$

Solutions of (3.5) for the typical value $\nu = 1/3$ are given in Figure1(a). Here, for each $1/3 = \rho_{min} < \rho < \rho_{max} = 5/3$, there are three branches of roots. The branch $m = m_{c2} > 0$, that emanates from $m = 2$ at $\rho = 0$ corresponds to a locus of Hamiltonian-Hopf points. This branch reaches an end point at $\rho = \rho_{max}$ by forming a limit point with another branch $m = m_{c1}$, which emanates from $m = 0$ in the integrable case, and corresponds to a curve of pairs of double real eigenvalues; i.e. eigenvalues of the form $-\lambda$ (twice) and λ (twice). This is not a bifurcation in the classical sense, but corresponds to the transition at $P = -2$ for the strut problem. Thus we have that the eigenvalues form a complex quadruple for $m_{c1} < m < m_{c2}$ (see Fig. 1(b)). On the highest branch, $m = m_{c3}$, there is a bifurcation caused by two zero eigenvalues (see the Fig. 1(b) for the implications of this for $\rho < \rho_{max}$). This curve of steady-state bifurcations emanates from infinity at $\rho = \rho_{min} = 1/3$, and there is a quadratic tangency between the top two curves at $\rho = \rho_c = 1.106395$, at which point all eigenvalues are zero.

For a general value of the ratio ν, we have the same qualitative picture as Fig. 1, including the tangency between m_{c_2} and m_{c_3}, but with

$$\rho_{min} = \nu, \quad \rho_c = \frac{3\nu^2 - 1\sqrt{9\nu+5}\,(1+\nu)^{(3/2)}}{2+4\nu}, \quad \rho_{max} = 1 + 2\nu.$$

Thus we have identified two codimension-two points which warrant further investigation; which occur as m varies for $\rho = \rho_c$ and $\rho = \rho_{max}$. A normal form respective to the former codim 2 point has been partially analysed by Iooss (1992).

(**a**)

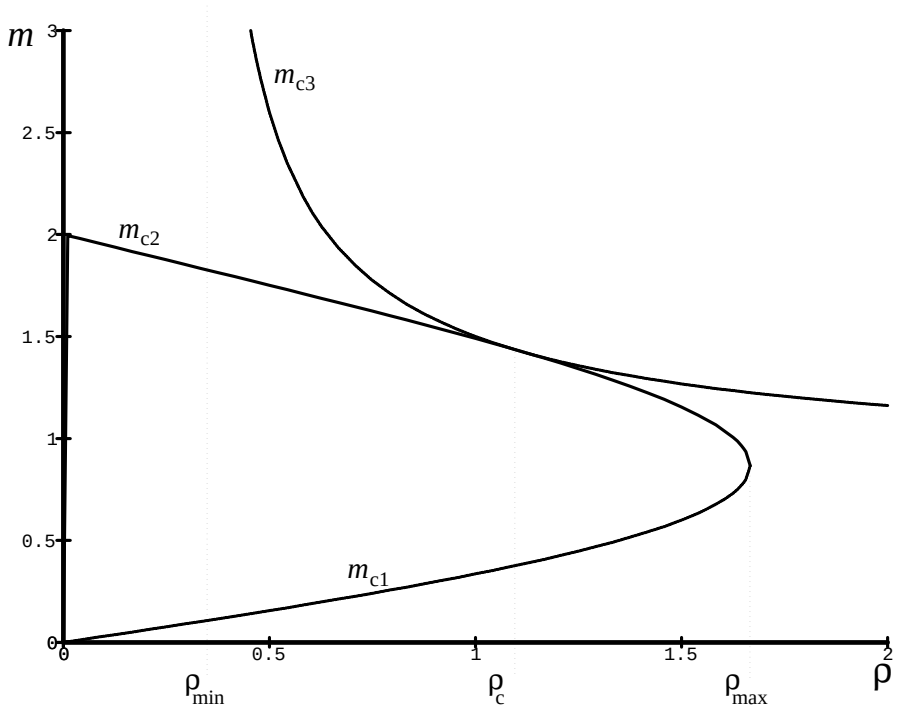

(**b**)

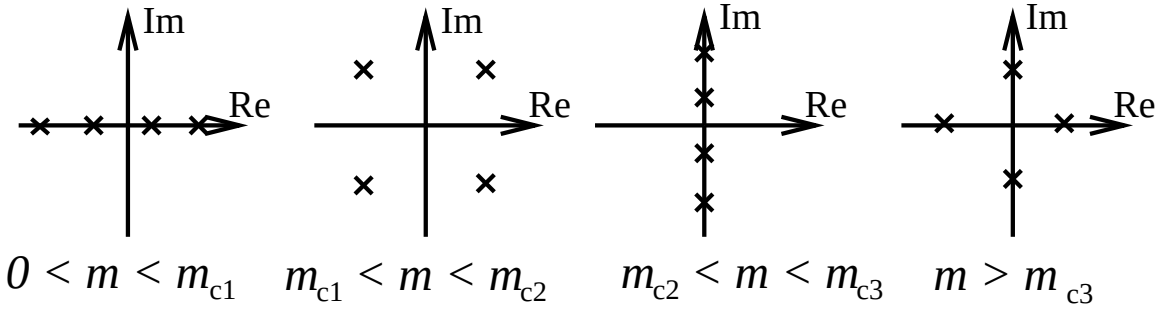

Figure 1: (a) Loci m_c of bifurcation points against ρ in Case 3 with $\nu = 1/3$, see text for interpretation of curves; (b) the non-trivial eigenvalues of the linearisation about **0** for a typical value of $\rho_{min} < \rho < \rho_{max}$.

3.2 Symmetry and multiplicity of homoclinic orbits

Recall from §2.5 that (2.13) may be regarded as a Hamiltonian system in a four-dimensional phase space. Moreover, as mentioned in the §2.6, in Cases 1 and 2 (2.13) completely integrable. As a consequence of this, for $m < m_c$ when the origin is a saddle-focus, it is known that the unstable manifold of the origin coincides with the two-dimensional stable manifold, giving a one-parameter family of homoclinic solutions. Computations of solutions in this one-parameter family are presented in §4 below.

Breaking the circular symmetry, by introducing non-zero ρ (Case 3), was shown by Mielke & Holmes (1988) to lead to isolated homoclinic orbits which represent *transverse intersections* of the stable and unstable manifolds of $\mathbf{0}$. The result of Devaney (1976*a*) (see also Wiggins (1988, p. 275)) applied to such a homoclinic orbit implies the existence of spatial chaos via the explicit construction of Smale horseshoes. Of more importance to us, although not stated explicitly by Devaney or Mielke & Holmes, is the existence of infinitely many extra *multi-modal* homoclinic orbits implied by the construction (see (Belyakov & Shil'nikov 1990, Buffoni et al. 1994), see also §4.4 below for the computation of such solutions for the present model). Note that Mielke & Holmes' is a local perturbation result valid for small ρ. However, transversality, the only additional requirement for Devaney's theory to apply, is a generic phenomenon for homoclinic orbits to saddle-focus equilibria in Hamiltonian systems.

An important feature of (2.13) is that, independent of the values of the constants ρ, a_i and b_i, it is invariant under two different transformations

$$R1 \quad : \quad (x_1, x_2, x_3, x_4, x_5, x_6) \to (-x_1, x_2, x_3, -x_4, x_5, x_6) \quad t \to -t, \tag{3.6}$$

$$R2 \quad : \quad (x_1, x_2, x_3, x_4, x_5, x_6) \to (x_1, -x_2, x_3, x_4, -x_5, x_6) \quad t \to -t. \tag{3.7}$$

For these transformations to define a *reversibility* in the sense of (Devaney 1976*b*), we require that the dimension of the set that is fixed by the transformation is half that of the underlying phase space. Recalling the result that solutions of (2.13) with given $|\mathcal{F}|$ and $\langle \mathcal{F}, \mathcal{G} \rangle$ may be viewed as evolving according to a four-dimensional dynamical system, we see that $R1$ and $R2$ do indeed define reversibilities in the classical sense. For transverse homoclinic orbits to saddle-focus homoclinic orbits in systems which are reversible, it is known (Champneys 1994, Härterich 1993) that there will be infinitely many multi-modal homoclinic orbits that are *symmetric*, that is invariant under the reversibility. This observation will prove useful in the numerical computations that follow.

Also, Iooss & Peroueme (1993) have analysed the normal form for a Hamiltonian-Hopf bifurcation in a reversible system. They showed that if a certain coefficient of the normal form is negative then, generically, a pair of symmetric small-amplitude homoclinic orbits bifurcate subcritically at the Hamiltonian Hopf bifurcation (that is, they exist for $m < m_c$ in the present context). Here, though, if such a condition holds we should expect the bifurcation of *four* small amplitude homoclinic orbits; one pair for each of the transformations (3.6) and (3.7). Again, if these orbits satisfy a transversality condition, there will exist infinitely many multi-modal homoclinic orbits (localized buckling modes) in the vicinity of the Hamiltonian Hopf point. By computing just such solutions in §4.4 below, we present strong *a posteriori* numerical evidence that the normal-form and transversality conditions do hold for a non-zero value of $\rho < \rho_{max}$.

Furthermore, the system (2.13) is $\mathbf{Z}_2$-symmetric, independent of the values of the physical

parameters. Specifically, it is invariant under the transformation

$$Z \quad : \quad (x_1, x_2, x_3, x_4, x_5, x_6) \to (-x_1, -x_2, x_3, -x_4, -x_5, x_6). \tag{3.8}$$

Note that this transformation defines a *symmetry* rather than a reversibility and implies that all orbits not in the invariant subspace $\{x_1 = x_2 = x_4 = x_5 = 0\}$ must either be themselves symmetric (i.e invariant under Z and a time shift) or come in pairs that are the images of each-other under Z (see, e.g., Golubitsky & Schaeffer (1985)). Note from (2.13), however, that if $x_i(\hat{t}) = 0$ for $i = 1, 2, 4, 5$ at some time $\hat{t}$, then $\dot{\boldsymbol{x}}(\hat{t}) = \mathbf{0}$ and hence $x_i(t) \equiv 0$ for all t. The only such solutions are given by $x_3 = \text{const.}$, $x_6 = \text{const.}$ and correspond to the trivial equilibrium position at different applied loads M and T. Hence, we have that all non-trivial solutions must occur in pairs, being images of each other under Z. This symmetry has a simple interpretation in terms of the physical space variables $\boldsymbol{r}(t)$. It corresponds to a half-rotation about the z-axis (the centerline of the unstrained rod). For Cases 1 and 2, where the cross-section of the rod is circular ($\rho = 0$), this is just one example of the wider symmetry of arbitrary rotations of the equations about the z-axis. In case 3, the symmetry is again obvious on physical grounds; one can rotate a tape through 180^o and find exactly the same equations.

It is not clear, without further analysis, whether the two reversible homoclinic orbits predicted by the normal form for a given reversibility will be images of each other under Z or not. If they were not, then we would expect the local birth of eight, rather than four, reversible homoclinic orbits from the Hamiltonian Hopf bifurcation when $\rho \neq 0$.

4 Numerical Results

4.1 Boundary Conditions

In order to compute localized buckling responses, we shall treat the dimensionless load parameter m as prescribed and look for solutions to (2.13) with $t \in (-\infty, \infty)$, satisfying the homoclinic boundary conditions

$$\boldsymbol{x} = (x_1, x_2, x_3, x_4, x_5, x_6) \to \mathbf{0} \quad \text{as} \quad t \to \pm\infty.$$

Computations on an infinite interval are not feasible, and so we truncate to a finite interval $t \in [0, \mathcal{T}]$, and apply approximations to the asymptotic boundary conditions, described as follows. For (2.13), with $0 < m < m_c$ (or $0 < m < m_{c3}$ in Case 3), the trivial equilibrium has eigenvalues of the form

$$0, 0, \pm\lambda \pm i\omega$$

($\lambda, \omega > 0$). An appropriate left-hand boundary condition is then

$$x_3(0) = x_6(0) = 0, \quad L_s(m)\boldsymbol{x}(0) = \mathbf{0} \tag{4.1}$$

(cf. Beyn (1990) and references therein), where $L_s(m)$ is the *projection* matrix onto the *left* eigenspace corresponding to the stable eigenvalues $-\lambda \pm i\omega$. This boundary condition places the solution in the unstable eigenspace of $\mathbf{0}$. An appropriate right-hand boundary condition

for reversible homoclinic orbits would be to place the solution in the symmetric section (fixed-point set) of either of the reversing transformations (Champneys & Spence 1993). Thus, the boundary conditions

$$x_1(\mathcal{T}) = x_4(\mathcal{T}) = 0, \tag{4.2}$$

$$x_2(\mathcal{T}) = x_5(\mathcal{T}) = 0 \tag{4.3}$$

specifically pick up solutions which are invariant under $R1$ or $R2$ respectively. Alternatively, we can pose boundary conditions analogous to (4.1) that place $\boldsymbol{x}(\mathcal{T})$ in the linearised eigenspace corresponding to the stable eigenvalues of $\mathbf{0}$.

When trying to understand the nature and multiplicity of homoclinic solutions it is often easier and instructive to solve an initial-value problem, i.e. to specify a six-dimensional initial condition for (2.13). In that case, we can explicitly place $\boldsymbol{x}(0)$ in the unstable eigenspace by setting

$$\boldsymbol{x}(0) = \epsilon(v_1 \cos\delta + v_2 \sin\delta), \tag{4.4}$$

where $v_1 \pm iv_2$ are the eigenvectors corresponding to $\lambda \pm i\omega$, ϵ is small, and $0 \leq \delta < 2\pi$.

In order to compute load-deflection bifurcation diagrams for localizing solutions, it is necessary to measure the end displacement D and end rotation R from the trivial straight-rod position at that value of m. When doing the computations we always think of m as fixed and D and R as passive. Of course, load-deflection diagrams so computed can always be interpreted for other loading sequences (Thompson & Champneys 1995). To measure dimensionless end displacement $\tilde{D} = DM/B$ and end rotation R, we solve (2.16) and (2.17) subject to the initial conditions

$$\tilde{\boldsymbol{r}}(0) = (0,0,0), \quad \boldsymbol{e}_1(0) = (1,0,0), \quad \boldsymbol{e}_2(0) = (0,1,0), \quad \boldsymbol{e}_3(0) = (0,0,1),$$

in tandem with (2.13), and take

$$\tilde{D} = \mathcal{T} - \tilde{r}_3(\mathcal{T}), \quad R \,(\mathrm{mod}\, 2\pi) = \arccos(< \boldsymbol{e}_1(\mathcal{T}), (1,0,0) >). \tag{4.5}$$

4.2 Case 1: circular cross-section linear rod

We begin by computing the Coyne localizing solution for $\rho = 0$, $\tilde{\eta} = \tilde{\mu} = 1$. Note that this one-dimensional manifold of homoclinic solutions to (2.13) is contained in the three-dimensional subspace given by taking the constants of integration 1, 1 and 0 in (2.18), (2.19) and (2.21) respectively. Henceforth we shall fix Poisson's ratio to be $\nu = 1/3$.

Numerically obtained solutions are depicted in Figs. 2–4, which were all obtained by solving an initial-value problem with initial conditions given by (4.4), with $\epsilon = 10^{-5}$ or smaller. Fig. 2 shows the evolution of a typical trajectory in the homoclinic manifold (defined by setting $\delta = 0$ in (4.4)) as the load parameter m is decreased. The solutions are depicted in physical space co-ordinates by solving (2.16) and (2.17) in tandem with (2.13). Fig. 3, which was obtained by taking eight different values of δ in (4.4), gives an idea of the shape of the homoclinic manifold in spatial co-ordinates for $m = 1.9$. Note that these solutions may be obtained analytically in closed form, using the formulae in Coleman et al. (1993) derived for solitary traveling waves.

Fig. 4 shows four of the solutions in Fig 3 as graphs of the phase-space variables x_i against arclength t. Figs. 4(a) and 4(b) show the non-dimensionalised forces (defined by x_1–x_3) and

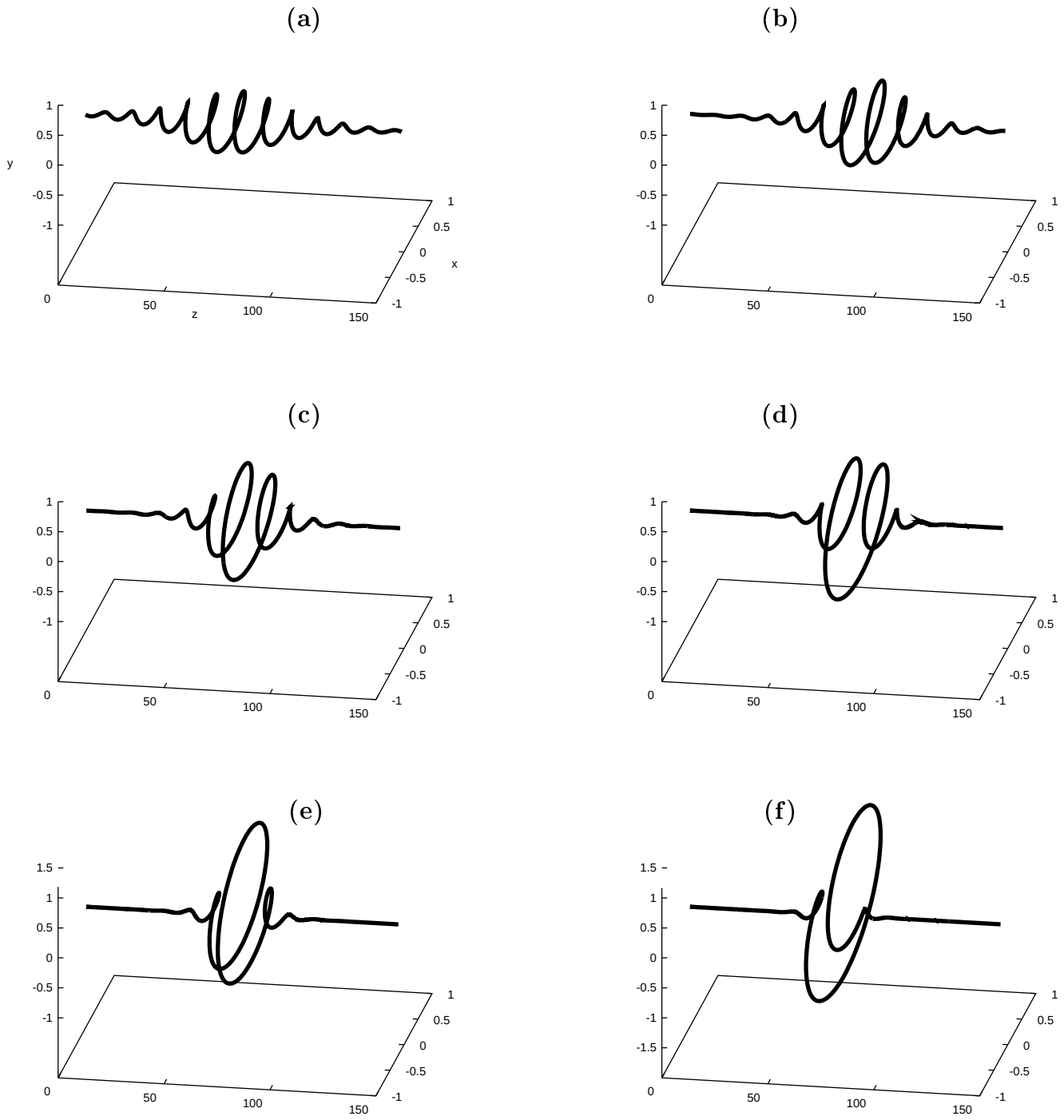

Figure 2: Evolution of the localized helix in Case 1 for (a) $m = 1.99$, (b) $m = 1.98$, (c) $m = 1.96$, (d) $m = 1.93$, (e) $m = 1.9$ and (f) $m = 1.8$.

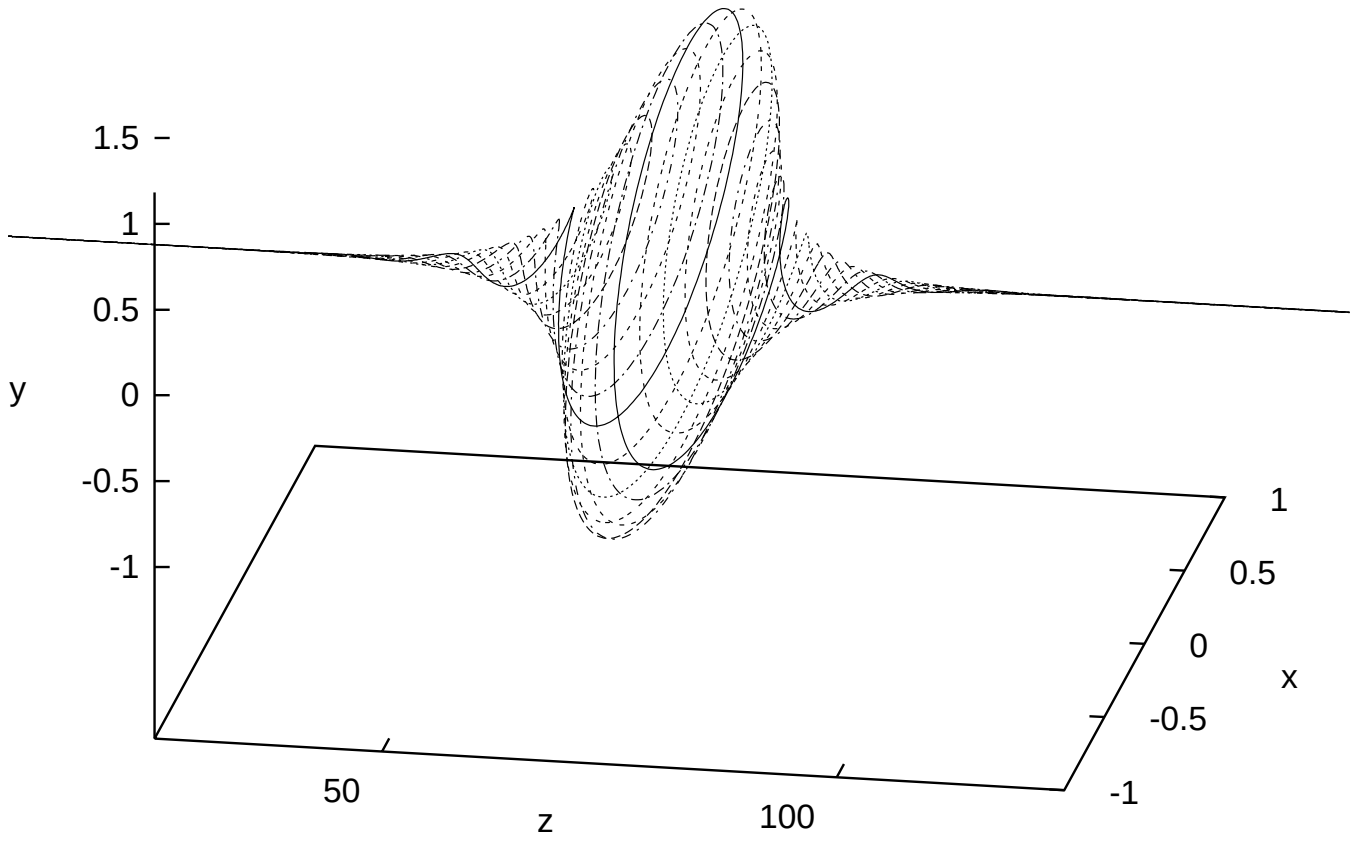

Figure 3: The manifold of homoclinic solutions in Case 1 at $m = 1.9$.

moments (defined by x_4–x_6) respectively along the rod, for a single initial condition. Note that $x_6(t) \equiv 0$, owing to (2.21). Also note that $x_3(t)$ is a non-oscillatory function that has a minimum at the mid-point of the localizing solution (i.e. at maximum deflection). Note also that $x_3(t)$ is the same function for all solutions within the manifold of homoclinic solutions at this parameter-value. However, as shown in Figs. 4(c)–(f), the functions $x_1(t)$, $x_2(t)$, $x_4(t)$, and $x_5(t)$ vary between solutions in the manifold. Note, with reference to (c) and (d) that there are precisely two solutions which have a minimum or maximum of x_1 and x_4 simultaneously at the mid-point of the rod (where x_3 has a minimum). These solutions are invariant under $R1$ and will prove important in §4.4 below. Similarly, there are precisely two solutions with extrema of x_2 and x_5 at the mid-point, and these are invariant under $R2$.

4.3 Case 2: nonlinear constitutive relations

Fig. 5 was computed in exactly the same way as Fig. 2 but with the softening nonlinear constitutive relations defined by $b_7 = b_8 = -1$. Note that the qualitative results are the same, but that the amplitude of the buckling mode grows much more rapidly with m for the present results (for example, compare figs. 2(f) with 5(d) which are for the same m-value). Qualitative similarities between solutions (although not the homoclinic case considered here) with linear and nonlinear constitutive laws were also found by Antman & Jordan (1974).

Fig. 6 shows bifurcation diagrams of end rotation R (mod 2π) and dimensionless end displacement $\tilde{D}$ against load m for the localizing solutions in Figs. 2 and 5. Note that $\tilde{D}$ and R are invariant for all solutions in the homoclinic manifold at a given m-value. Observe from Fig. 6 that end displacement is unaffected by the softening, but that there is a rapid increase in end-rotation for a given load in Case 2 compared with the linear constitutive laws (in order to plot the two curves in Fig. 6(b), we have shifted the dashed curve downwards through 2π).

4.4 Case 3: non-circularly-symmetric rods

We now consider the non-integrable case of a rod with linear constitutive laws but with a non-circular cross-section. Specifically, we shall take $\rho = 0.5$. For this value of ρ the two Hamiltonian-Hopf bifurcations occur at $m_{c_1} = 0.155739$ and $m_{c_2} = 1.751187$. We shall consider solutions at $m = 1.7$, which is just below the value at which the higher Hamiltonian-Hopf bifurcation occurs. Hence we are in the subcritical region into which the homoclinic orbits given by the normal-form theory would emanate. All computations were performed with $\epsilon = 10^{-5}$ in (4.4).

Fig. 7 shows what happens for two randomly-chosen values of the angle δ in the initial conditions (4.4). These solutions appear spatially chaotic (but, of course, do not satisfy the asymptotic right-hand boundary condition). Thus we no longer have the situation that all solutions in the unstable manifold of $\mathbf{0}$ are homoclinic. Instead, any homoclinic trajectory should generically be isolated and represent the transverse intersection of stable and unstable manifolds.

Fig. 8–11 show four homoclinic orbits computed using a shooting algorithm that varies the value of δ in (4.4) in order to satisfy one of the right-hand boundary conditions (4.2) or (4.3) (Champneys & Spence 1993). Fig. 8 shows the four orbits predicted by the normal-form theory recalled in §3.2; which we shall call the *primary* homoclinic buckling modes. Data relating to

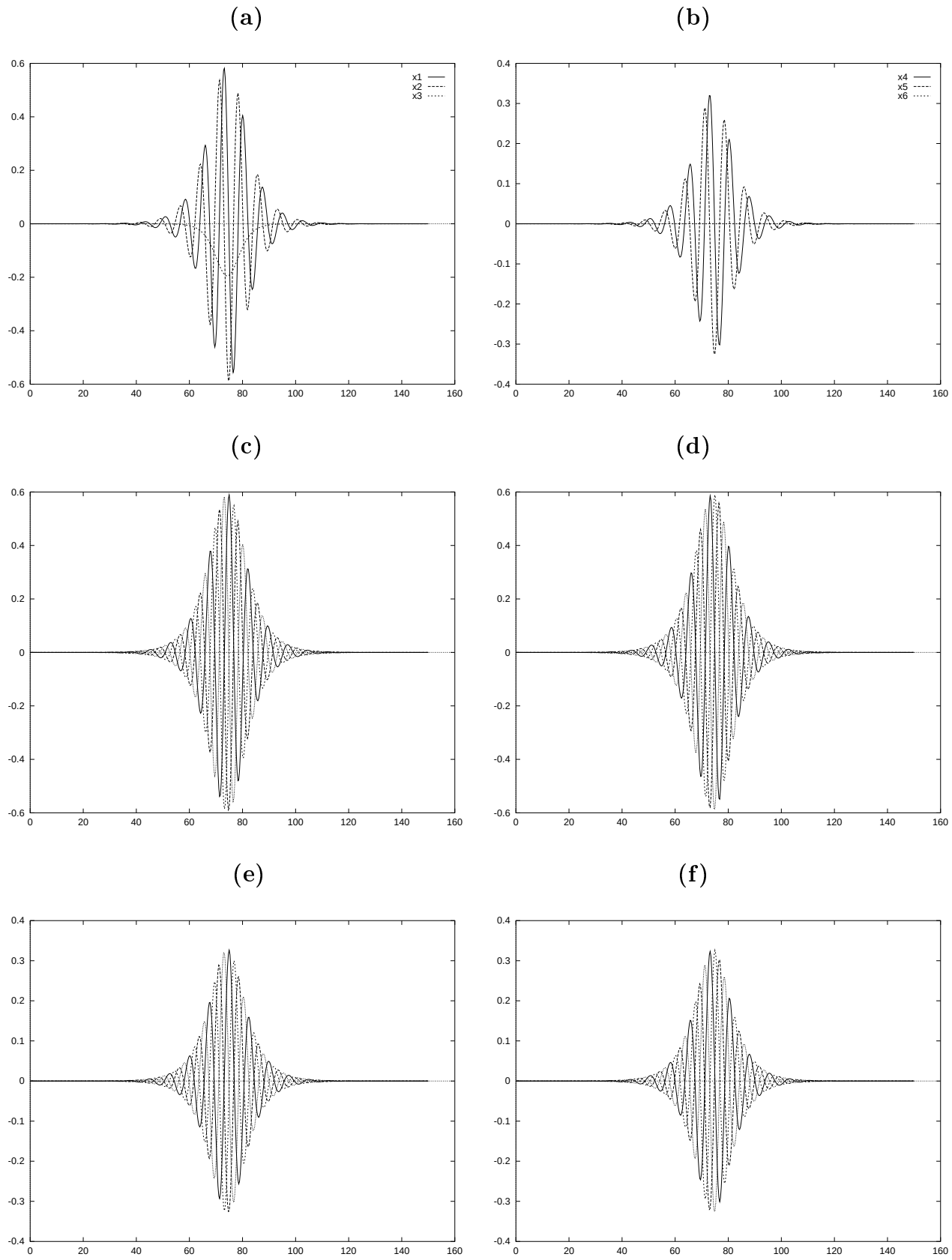

Figure 4: Forces and moments against arclength for the solutions in Fig. 3 at $m = 1.9$. (a), (b) x_1—x_6 for a single orbit. (c)–(f) Four representative solutions in the manifold: (c) x_1 against t, (d) x_2 against t, (e) x_4 against t, (f) x_5 against t.

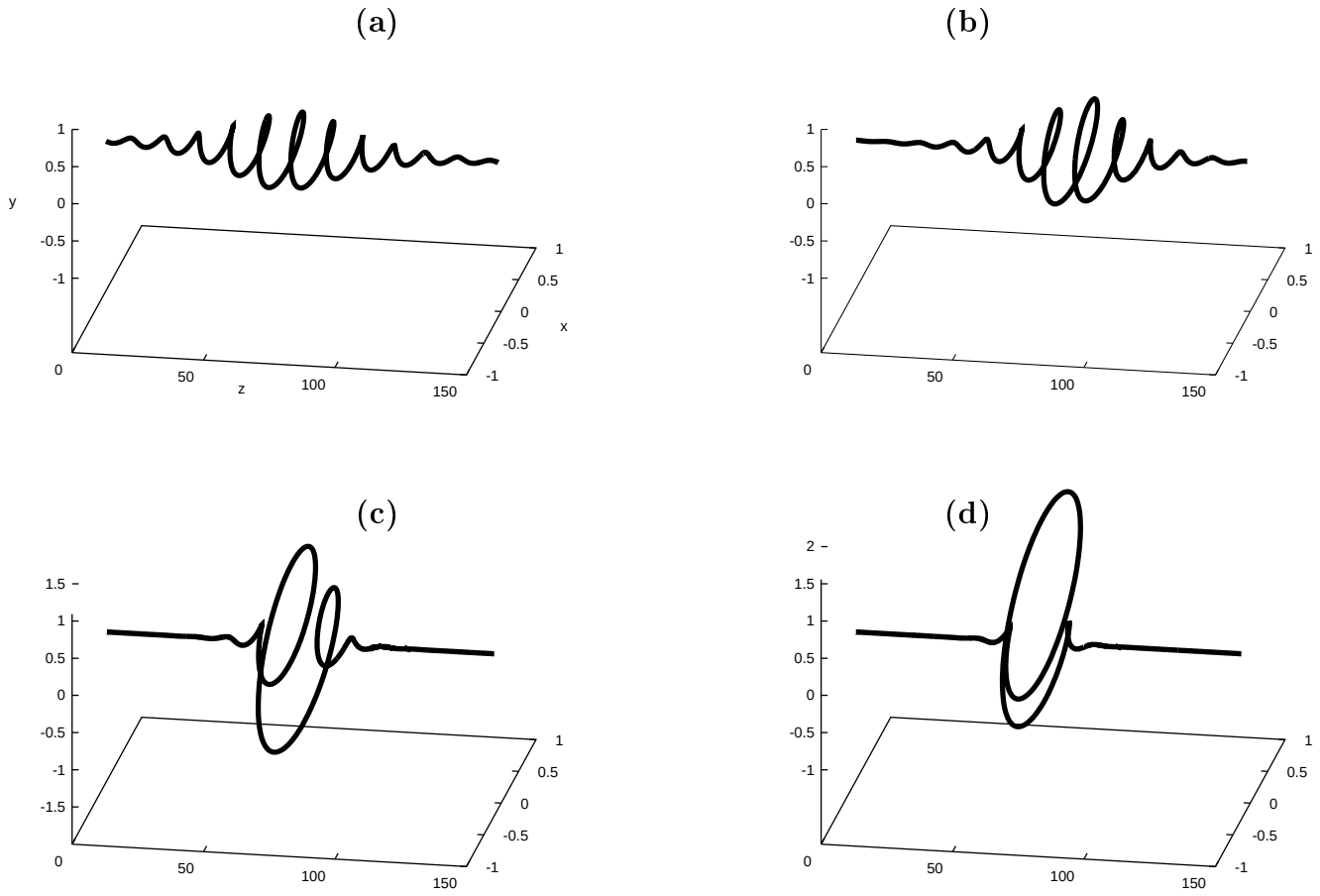

Figure 5: Evolution of the localized helix in Case 2 with $b_7 = b_8 = -1$ for (a) $m = 1.99$, (b) $m = 1.98$, (c) $m = 1.9$ and (d) $m = 1.8$

Figure	δ	*Mid-point* $\mathcal{T}$	*Modality*	*Reversible under*	*Image under* Z
10(a)	6.0664	71.4986	primary	$R1$	10(b)
10(b)	2.9248	71.4986	primary	$R1$	10(a)
10(c)	1.3318	71.4674	primary	$R2$	10(d)
10(d)	4.4734	71.4674	primary	$R2$	10(c)
12(a)	6.2382	99.1416	bi-modal	$R1$	not depicted
12(b)	5.9794	101.0853	bi-modal	$R1$	not depicted
12(c)	0.1503	97.1052	bi-modal	$R2$	not depicted
12(d)	1.4985	99.1069	bi-modal	$R1$	not depicted
12(e)	1.3301	112.8061	bi-modal	$R2$	not depicted
12(f)	6.2457	125.5414	tri-modal	$R1$	not depicted

Table 1: Data relating to the computation of localized buckling solutions for $\rho = 0.5$ and $m = 1.7$, with $\epsilon = 10^{-5}$, $v_1 = (0.6964, 0.0563, 0.3810, -0.0413)$ and $v_2 = (0, 0.5422, 0.0857, 0.2524)$

(a)

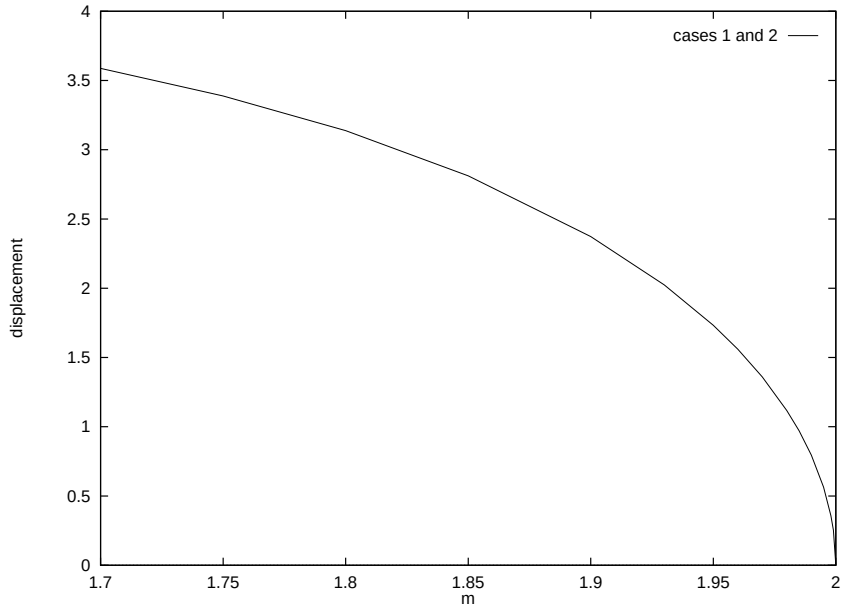

(b)

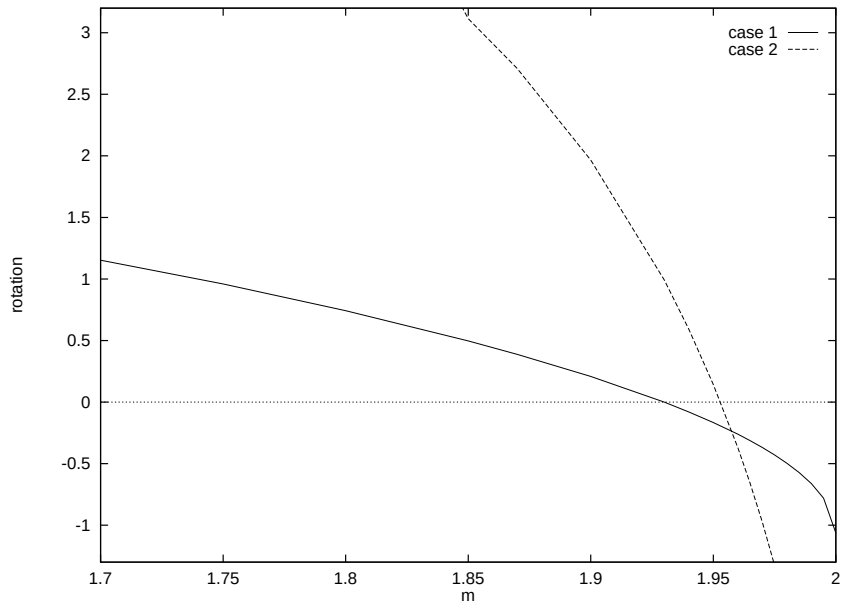

Figure 6: Numerically computed bifurcation diagrams of the localized mode in cases 1 and 2. (a) Load against end displacement. (b) Load against end rotation.

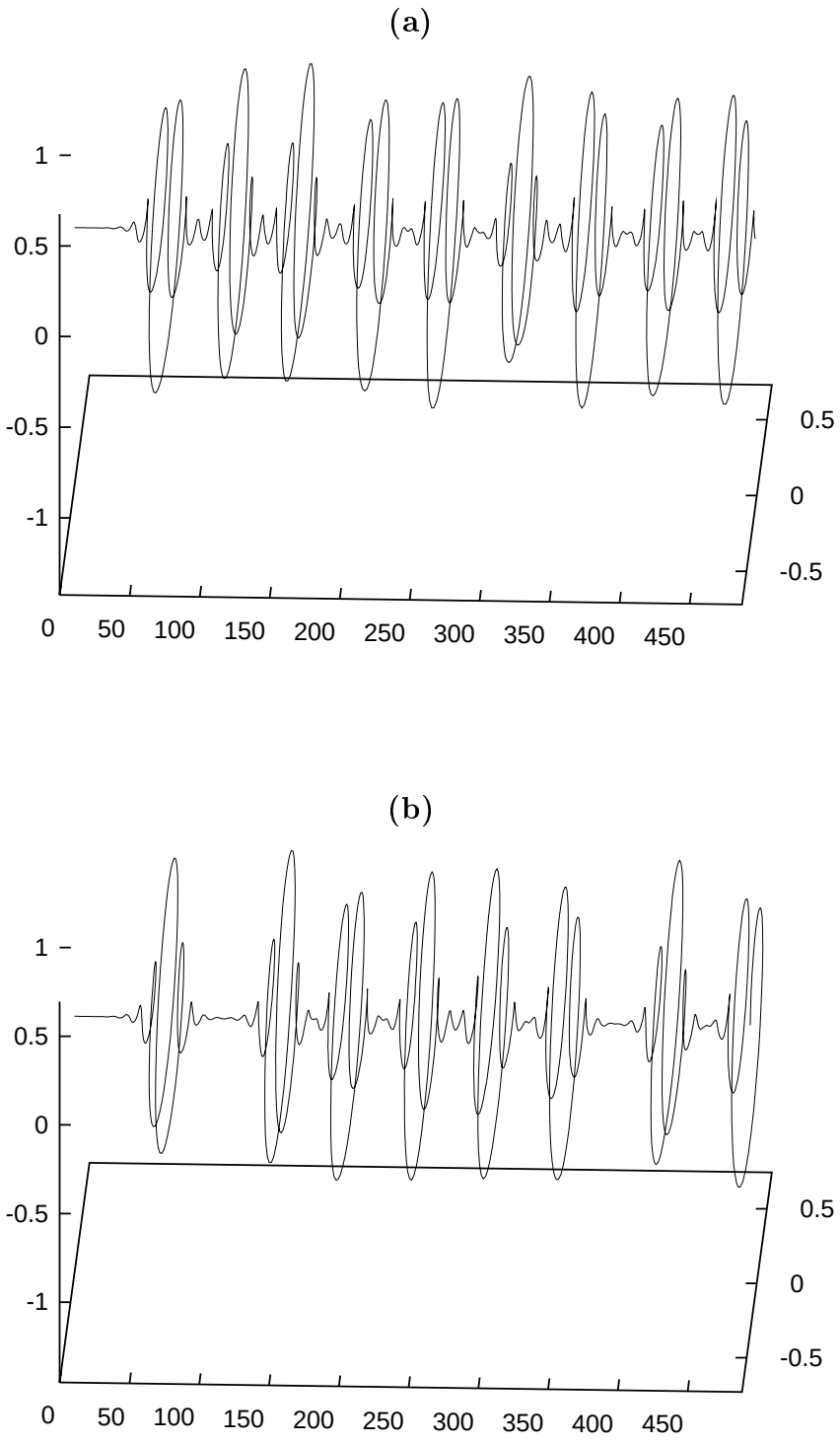

Figure 7: Two spatially chaotic solutions with linear constitutive relations and $\rho = 0.5$ at $m = 1.7$

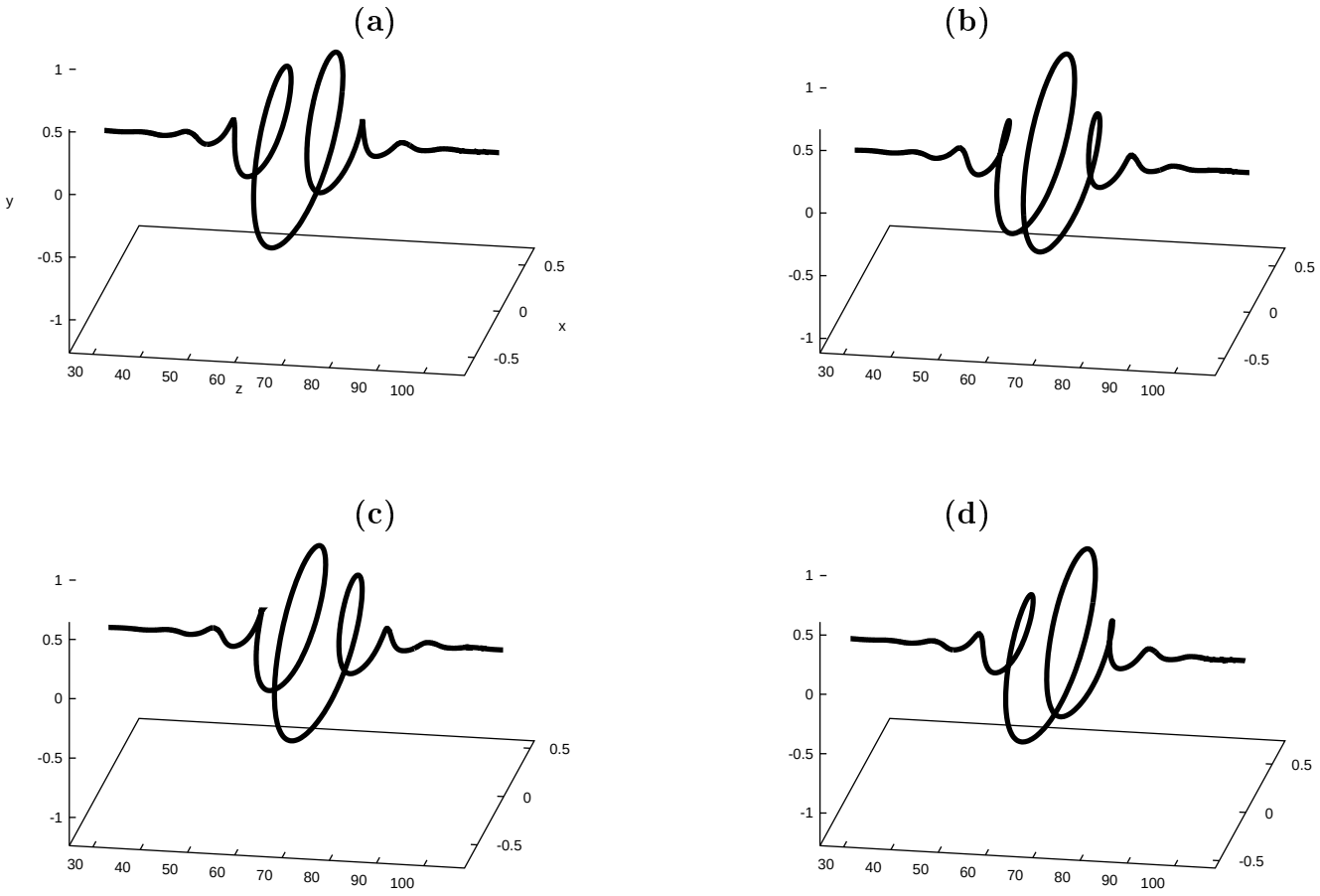

Figure 8: The four primary localized buckling modes for $\rho = 0.5$, $m = 1.7$

these orbits are given in Table 1. Note that the first two orbits presented, likewise the final two, are images of each other under the reflection Z. Consequently the values of δ for the two orbits of a pair differ by exactly π. The reversibility properties of the first and third orbits in Fig. 8 are elucidated in Fig. 9, where the components x_i are plotted against t. Note that the first one is reversible under R1 (see (3.7)) because $x_2(0) = x_5(0) = 0$ where $t = 0$ now represents the midpoint of the rod, and the second one is similarly reversible under R2 (see (3.6)).

Figs. 10 and 11 show some *multi-modal* homoclinic orbits computed at $m = 1.7$, data for each of which are summarised in Table 1. The fact that we have been able to compute these modes provides *a posteriori* evidence of the transverse intersection of stable and unstable manifolds along the primary orbits and that Devaney's theory recalled in §3.2 can be applied here to give *infinitely many localized buckling modes*. Note, with reference to Fig. 11, that we have here an even greater multiplicity of localized buckling modes than the theory applied to a single primary homoclinic orbit would suggest. As well as infinitely many bi-modal orbits that are like two copies of any given primary orbit (those in Fig. 11(a) and (b) are the first two in such a sequence relating to the primary orbit 10(a)), there are also *mixed-mode* bi-modal orbits (e.g. Fig. 11 (c) and (d)) that are like a copy of each of two distinct primary orbits. Clearly, there are even more possibilities when one considers tri-modal orbits (Fig. 11 (f)) and higher.

The numerical methods of Champneys & Spence (1993) could now be applied to (2.13) to systematically compute families of the localized buckling modes. Similarly, one could use AUTO (Doedel, Keller & Kernévez 1991), to path-follow representatives of the multitude of homoclinic solutions, as was performed for a simpler model of an elastic strut resting on a nonlinear foundation in Buffoni et al. (1994). Such a comprehensive numerical investigation is the subject of on-going work, but in the Conclusion which follows we indicate what one might expect in the light of what is known for the strut model.

5 Conclusion

This paper has focussed on a mathematical investigation, via the celebrated Kirchhoff analogy with an initial-value problem, of localized buckling in rods subject to end tension and moment. The significance of localized, rather than periodic buckling, for long rods was shown experimentally and analytically in the companion paper Thompson & Champneys (1995). Several unexplained theoretical issues arising from that paper need further investigation, not least the experimental observation of a perturbed one-twist-per wave mode H_1 in the pre-buckled state. From the structure of the Frenet-Seret equations (2.7), note that a one-twist-per wave mode in the Kirchoff-Love formulation corresponds to a non-trivial equilibrium of (2.13). A careful study is required of which perturbing influences, such as initial curvature, asymmetric loading, gravity inclusion of shear deformations, axial-extensibility and finite-radius effects can cause such non-trivial equilibria to occur.

For rods without circular symmetry in the cross-section, we have demonstrated in this paper that a realm of additional complexity enters the solution structure of the mathematical problem, even when one restricts attention to localizing solutions. We remark that there is a qualitative similarity with the known situation for a strut resting on a nonlinear elastic foundation, the vertical displacement u of which is given, in dimensionless form, by

$$\ddddot{u} + P\ddot{u} + u - u^2 = 0, \tag{5.1}$$

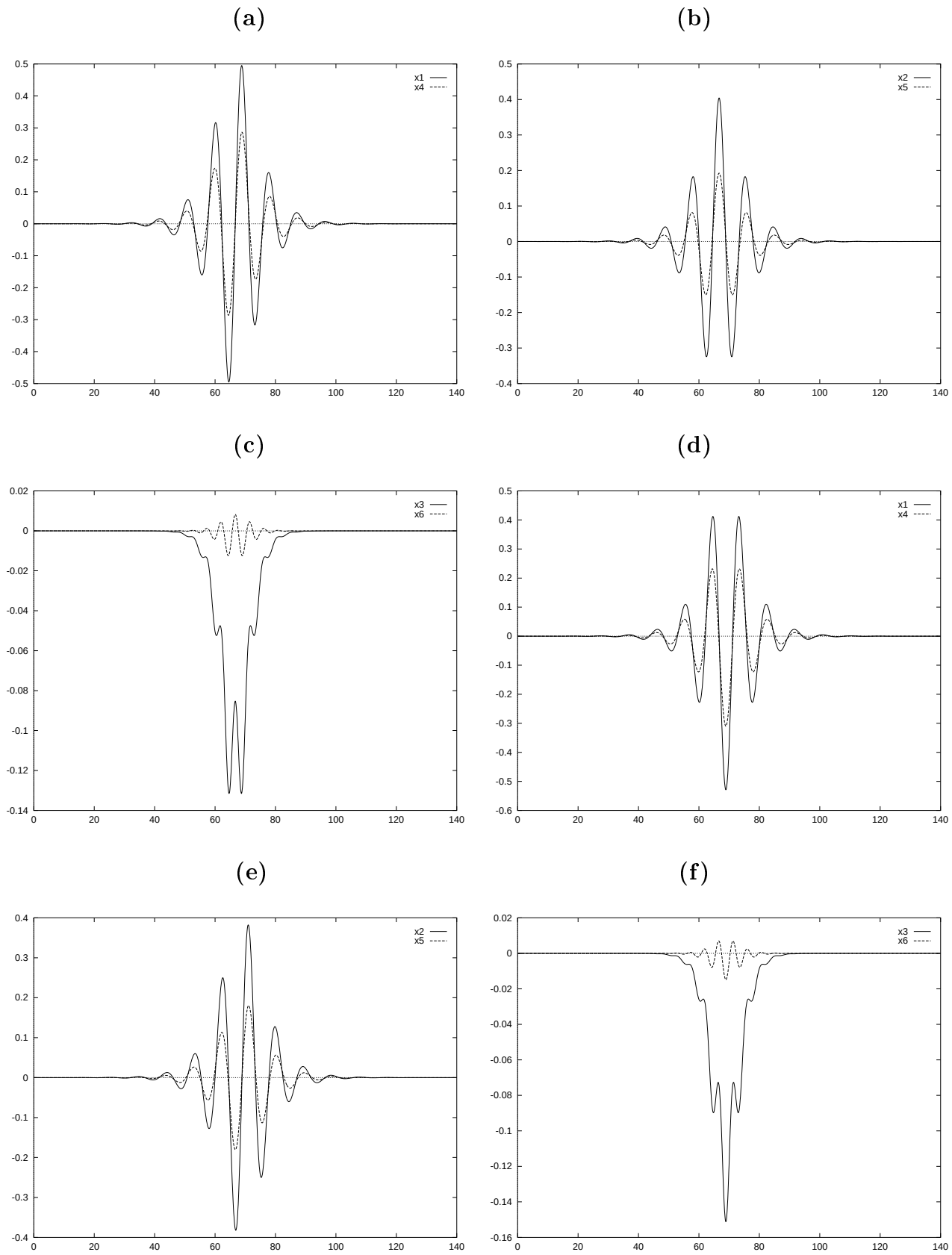

Figure 9: Forces and moments for (a)–(c) the first, and (d)–(f) the third orbit of Table 1

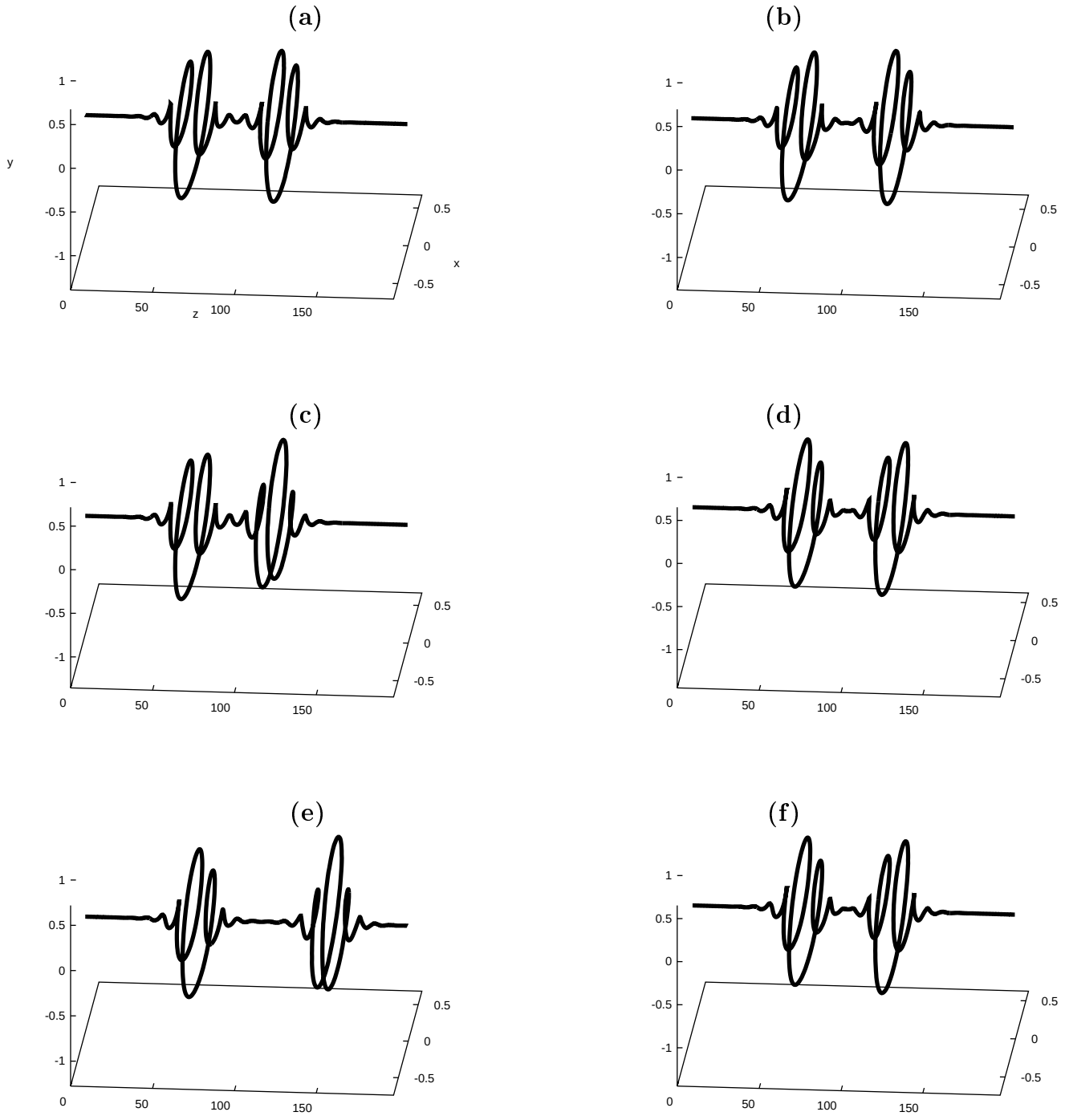

Figure 10: The spatial configuration of six multi-modal localized buckling modes for $\rho = 0.5$, $m = 1.6$

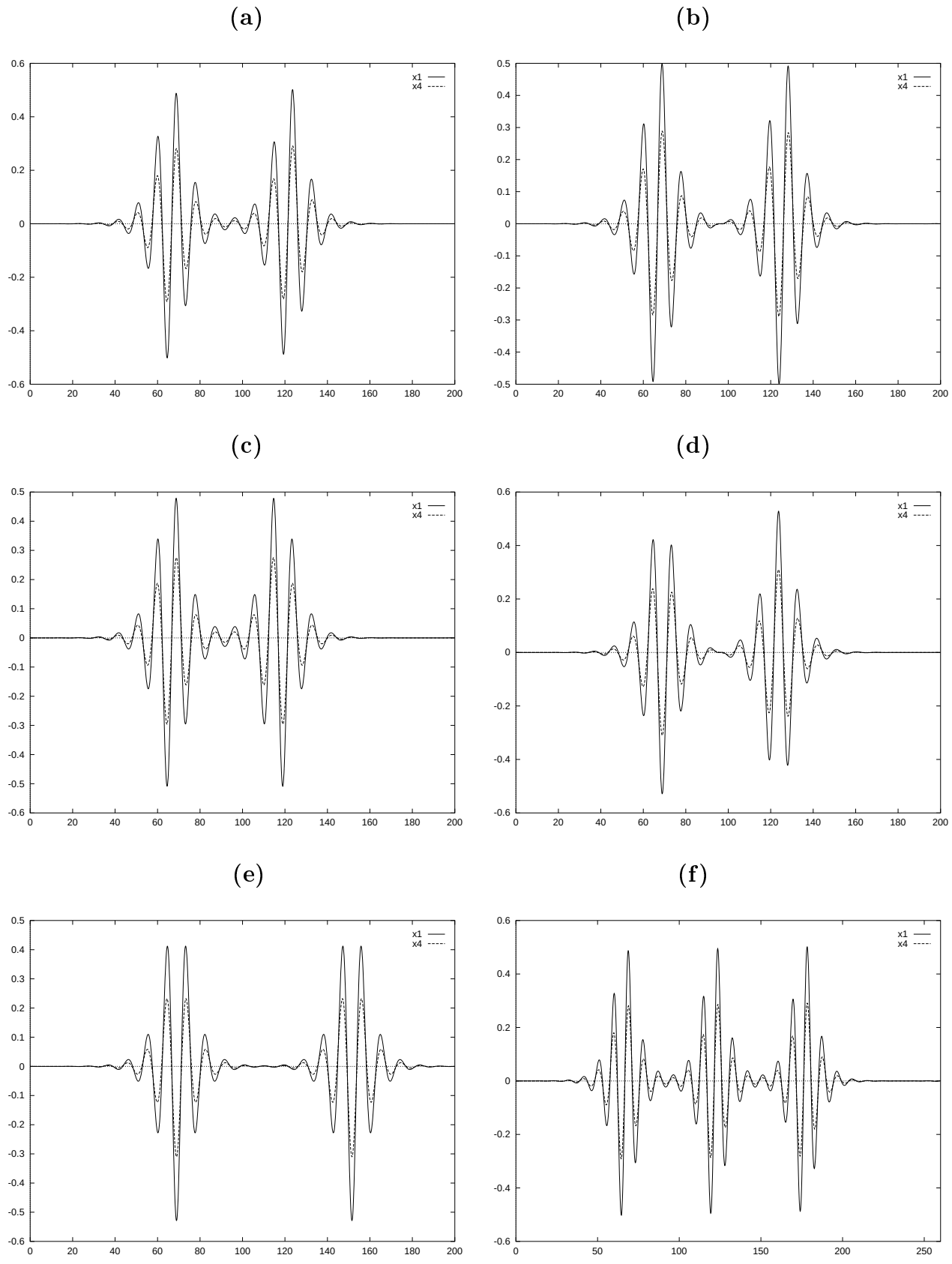

Figure 11: Second components of force and moment against t for each of the six multi-modal orbits depicted in the previous figure.

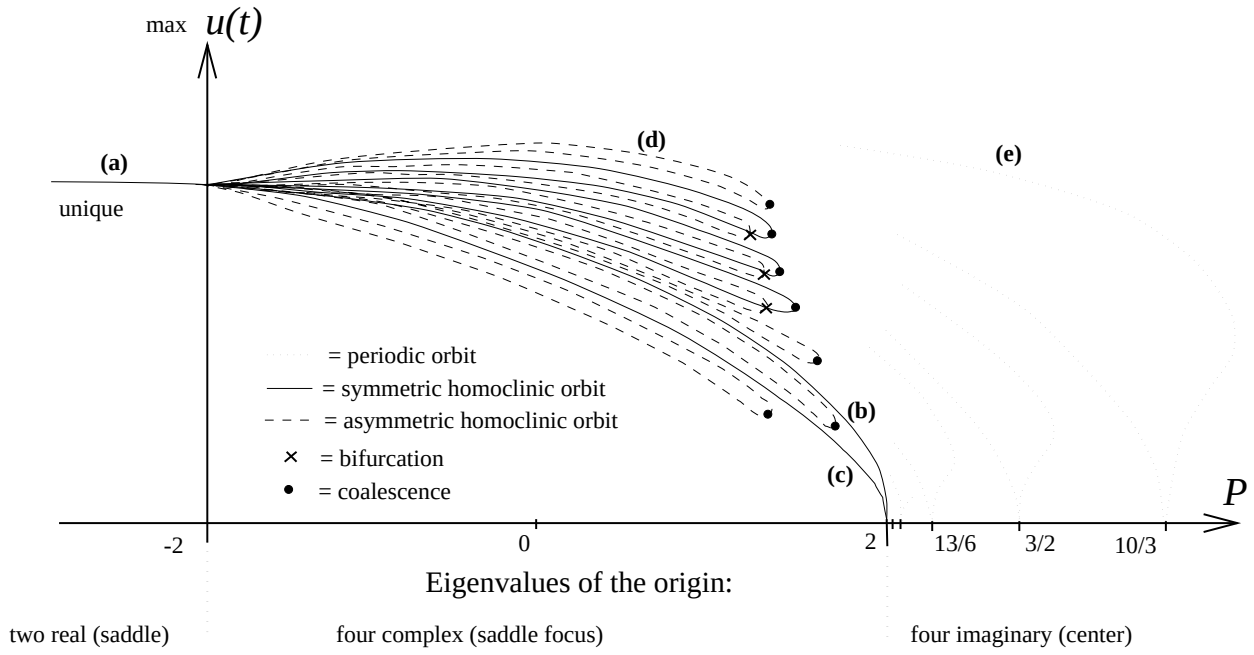

Figure 12: Schematic bifurcation diagram of a representative sample of periodic and homoclinic solutions of (5.1) for the strut on a nonlinear elastic foundation.

where a dot denotes differentiation by a dimensionless horizontal variable x (see (Hunt et al. 1989, Hunt & Wadee 1991) and references therein). The dynamical system corresponding to (5.1) is reversible under $t \to -t$ and, like (2.13), (5.1) depends on a single dimensionless load parameter, P. On varying P the eigenvalues of the trivial equilibrium undergo a sequence of transitions equivalent to the first three pictures of Figure 1(b), with the supercritical Hamiltonian-Hopf bifurcation occuring at $P = 2$ and m_{c1} corresponding to $P = -2$. Figures 12 and 13 summarise the known analytical and numerical results for the global behaviour of localized buckling modes of (5.1), which are collected in (Buffoni et al. 1994). The figures also present what is known about periodic orbits with zero value of the Hamiltonian, which relies on unpublished work by Toland (1992) that there is a bifurcation of two such solutions for $P = m/n + n/m$ for all integers m and n, and some numerical experiments by the first author.

We conjecture that an overall similar pattern of behaviour should be observed for the twisted rod problem for non-zero ρ. In particular, we expect that loci of multi-modal orbits upon increasing $m < m_c$ should undergo limit points, or *coalescences* with respect to m, with the coalescent solution at the limit point having a greater modality. Note also from Figures 12 and 13 that there also exist asymmetric multi-modal localized buckling modes, and that certain of these solutions bifurcate from symmetric modes immediately before the coalescence (see (Buffoni et al. 1994) for the details). We should expect similar bifurcations to occur for the twisted rod, because an examination of Devaney's theory for reversible systems predicts asymmetric as well as symmetric multi-modal solutions. Moreover, Knobloch (1994) has recently shown that such bifurcations and coalescences are generic codim 1 bifurcations of homoclinic solutions in reversible Hamiltonian systems. However, as highlighted in §4.4, there is an even greater multiplicity of localizing solutions for (2.13), due to the extra symmetry and reversibility. Not least because of this extra mathematical structure, there clearly remains a lot of work to be

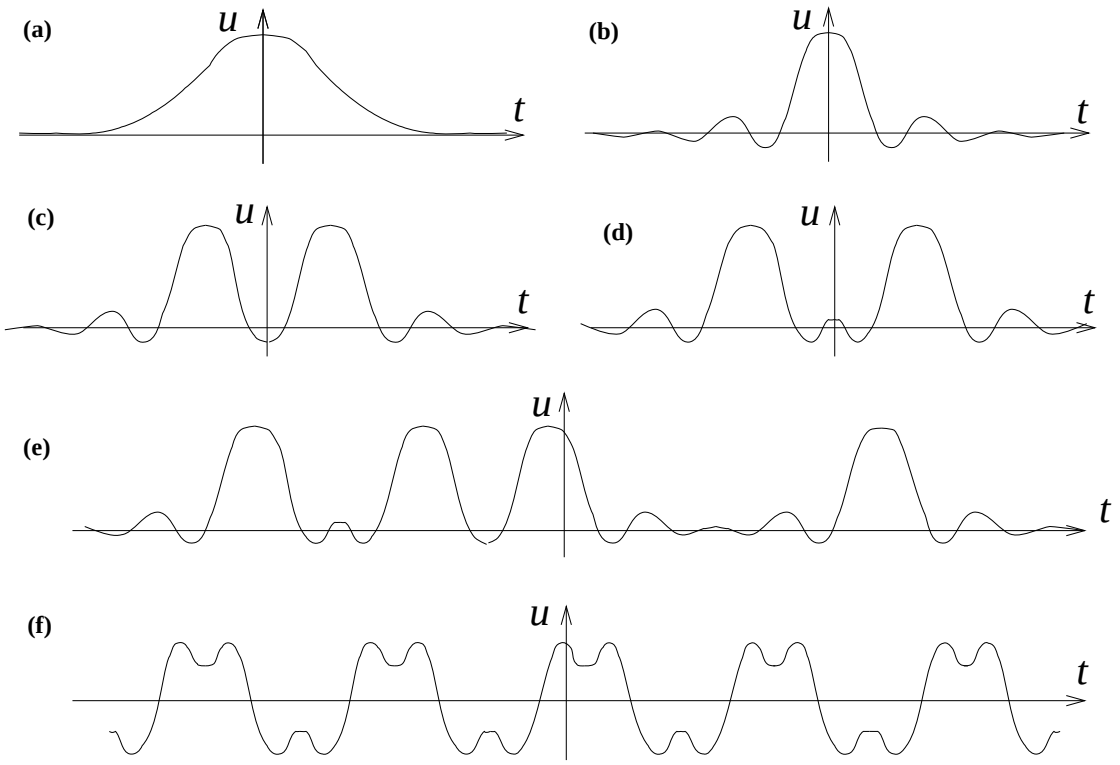

Figure 13: Schematic graphs of some of the solutions depicted in Fig. 13; (a) primary homoclinic orbit for $P < -2$, (b) primary orbit for $P > 0$, (c) bi-modal orbit that survives to $P = 2$, (d) another bi-modal orbit, (e) an asymmetric 4-modal orbit, corresponding to the integer sequence $(4, 2, 8)$, (f) one of the zero-energy periodic orbits emanating from the resonance at $P = 10/3$.

done before a comprehensive picture of localizing solutions to (2.13) emerges similar to that for the strut.

An additional complication for the rod is that there are more possibilities for the linear problem, depending on the parameter ρ. We have identified two codimension-two points of interest, which occur as m varies for $\rho = \rho_c$ and $\rho = \rho_{max}$. Beyond the latter ρ-value, the Hamiltonian-Hopf bifurcation disappears. The physical interpretation of these two points needs to be investigated. In fact, the complete bifurcation diagram of the linear problem, Fig. 3, is qualitatively the same as that for water waves in the presence of surface tension (Iooss & Kirchgässner 1992, Fig. (2.1)). Numerical continuation techniques should be used to see the effect of each of these parameter regions on the existence of localizing solutions. Finally, it would be nice to put our tentative statements on transversality and genericity on a mathematical rigorous framework, perhaps by using normal form theory applied at the codimension-two points, c.f. Iooss (1992).

It remains to be seen what the ramifications of our results on non-circular cross-section rods are for the outcomes of experiments. The major caveat to the approach adopted here of using a dynamical systems analogy is that no information is obtained about the physical stability of the computed localized buckling solutions. It would be interesting to see if under certain loading conditions, any of the multiplicity of multi-modal buckling modes can be stable, or meta-stable, solutions of the structural problem. A necessary condition for stability is that the equilibrium configuration minimises a potential energy functional. Variational methods, which take account of the different possible loading conditions should prove useful for answering questions about stability (cf. (Dichmann et al. 1993, Buffoni 1994, Maddocks & Sachs 1995) for example). Such an investigation is left for future work. Nonetheless, despite this obvious limitation of the method, regarding the equilibrium equations as a dynamical system with arclength playing the role of time, has enabled us to understand with very little effort the existence of a multitude of localized buckling solutions for the twisted rod problem.

Acknowledgments

We should like to thank Dr. Gert van der Heijden for carefully repeating our numerical results and finding some errors, and also an anonymous referee of an earlier version for drawing several additional references to our attention.

References

Amick, C. J. & Toland, J. F. (1992), 'Homoclinic orbits in the dynamic phase space analogy of an elastic strut', *European J. Appl. Maths.* **3**, 97–114.

Antman, S. S. & Jordan, K. B. (1974), 'Qualitative aspects of the spatial deformation of non-linearly elastic rods', *Proc. Roy. Soc. Edin. A* **73**, 85–105.

Antman, S. S. & Kenney, C. S. (1981), 'Large buckled states of nonlinearly elastic rods under torsion, thrust and gravity', *Arch. Rat. Mech. Anal.* **84**, 289–338.

Belyakov, L. A. & Shil'nikov, L. P. (1990), 'Homoclinic Curves and Complex Solitary Waves', *Selecta Mathematic Sovietica* **9**, 219–228.

Beyn, W.-J. (1990), 'The numerical computation of connecting orbits in dynamical systems', IMA *J. Num. Anal.* **9**, 379–405.

Buffoni, B. (1994), Periodic and homoclinic orbits for Lorenz-Lagrangian systems via variational methods, Submitted.

Buffoni, B. & Toland, J. F. (1994), Global bifurcation of homoclinic and periodic orbits for autonomous Hamiltonian systems, *J. Diff. Eq.* to appear.

Buffoni, B., Champneys, A. R. & Toland, J. F. (1994), Bifurcation and coalescence of a plethora of homoclinic orbits for a Hamiltonian system, Technical report, University of Bath.

Buffoni, B., Groves, M. & Toland, J. (1995), A plethora of solitary gravity-capillary water waves with nearly critical bond and froude numbers., Mathematics Preprint, University of Bath.

Buzano, E., Geymonat, G. & Poston, T. (1985), 'Post-buckling behaviour of a non-linearly hyperelastic thin rod with cross-section invariant under the dihedral group D_n', *Arch. Rat. Mech. Anal.* **89**, 307–388.

Champneys, A. R. (1994), 'Subsidiary homoclinic orbits to a saddle-focus for reversible systems', *Int. J. Bifurcation Chaos* **4**, 1447–1482.

Champneys, A. R. & Spence, A. (1993), 'Hunting for homoclinic orbits in reversible systems: a shooting technique', *Adv. Comp. Math.* **1**, 81–108.

Champneys, A. R. & Toland, J. F. (1993), 'Bifurcation of a plethora of multi-modal homoclinic orbits for autonomous Hamiltonian systems', *Nonlinearity* **6**, 665–721.

Coleman, B., Dill, E., Lembo, M., Lu, Z. & Tobias, I. (1993), 'On the dynamics of rods in the theory of Kirchoff and Clebsch', *Arch. Rat. Mech. Anal.* **121**, 339–359.

Coyne, J. (1990), 'Analysis of the formation and elimination of loops in twisted cable', *IEEE J. Oceanic Eng.* **15**, 71–83.

Davies, M. A. & Moon, F. C. (1993), '3-D spatial chaos in the elastica and the spinning top: Kirchhoff analogy', *Chaos* **3**, 93–99.

Devaney, R. L. (1976*a*), 'Homoclinic orbits in Hamiltonian systems', *J. Diff. Eqns.* **21**, 431–438.

Devaney, R. L. (1976*b*), 'Reversible diffeomorphisms and flows', *Trans. Amer. Math. Soc.* **218**, 89–113.

Dichmann, D., Maddocks, J. & Pego, R. (1993), 'Hamiltonian dynamics of an elastica and the stability of solitary waves'. Submitted to *Arch. Rat. Mech. Anal.*

Doedel, E. J., Keller, H. B. & Kernévez, J. P. (1991), 'Numerical analysis and control of bifurcation problems: (II) Bifurcation in infinite dimensions', *Int. J. Bifurcation and Chaos* **1**, 745–772.

Golubitsky, M. & Schaeffer, D. G. (1985), *Singularities and Groups in Bifurcation Theory; Volume I*, Springer-Verlag, Berlin.

Härterich, J. (1993), Kaskaden homokliner Orbits in reversiblen dynamischen Systemen, Master's thesis, Universität Stuttgart.

Hunt, G. W. & Wadee, M. K. (1991), 'Comparative lagrangian formulations for localized buckling', *Proc. R. Soc. Lond.* A **434**, 485–502.

Hunt, G. W., Bolt, H. M. & Thompson, J. M. T. (1989), 'Structural localization phenomena and the dynamical phase-space analogy', *Proc. R. Soc. Lond.* A **425**, 245–267.

Iooss, G. (1992), A codimension-two bifurcation for reversible vector fields, *in* 'Proc. Workshop on Normal Forms and homoclinic chaos', Fields Institute, Waterloo.

Iooss, G. & Kirchgässner, K. (1992), 'Water waves for small surface tension: an approach via normal form', *Proc. Roy. Soc. Edinburgh* **112 A**, 267–299.

Iooss, G. & Peroueme, M. C. (1993), 'Perturbed homoclinic solutions in reversible 1:1 resonance vector fields', *J. Diff. Eq.* **102**, 62–88.

Kirchhoff, G. (1859), 'Über das Gleichgewicht und die Bewegung eines unendlich dünnen elastischen Stabes', *J. für Mathematik (Crelle)* **56**, 285–313.

Knobloch, J. (1994), Bifurcation of degenerate homoclinics in reversible and conservative systems, Preprint No. M 15/94 Technische Universität Illmenau.

Lichtenberg, A. J. & Lieberman, M. A. (1992), *Regular and chaotic dynamics*, 2nd ed. edn, Springer-Verlag, Berlin.

Love, A. E. H. (1927), *A Treatise on the Mathematical Theory of Elasticity*, 4th ed. edn, Cambridge University Press, Cambridge.

Maddocks, J. & Dichman, D. (1994), 'Conservation laws in the dynamics of rods', *J. Elasticity* **34**, 83–96.

Maddocks, J. & Sachs, R. (1995), Constrained variational principles and stability in hamiltonian systems, *in* H. Dumas, K. Meyer & D. Schmidt, eds, 'Hamiltonian Dynamical Systems', The IMA Volumes in Mathematics and Its Applications, **63**, pp. 231–264.

Mahadevan, L. & Keller, J. B. (1993), 'The shape of a Mobius band', *Proc. R. Soc. Lond.* **440 A**, 149–162.

Mahadevan, L. & Keller, J. B. (1995), 'Periodic folding of thin sheets', *SIAM J. Appl. Math.*

Mielke, A. & Holmes, P. (1988), 'Spatially complex equilibria of buckled rods', *Arch. Rat. Mech. Anal.* **101**, 319–348.

Pierce, J. (1991), *Singularity theory and the buckling of rods*, Springer-Verlag, Berlin.

Thompson, J. M. T. & Champneys, A. R. (1995), 'From the helix to localized writhing in the torsional post buckling of elastic rods'. *Proc. Roy. Soc. Lond. A* accepted.

Thompson, J. M. T. & Virgin, L. N. (1988), 'Spatial chaos and localisation phenomena in nonlinear elasticity', *Phys. Lett. A* **126**, 491–496.

Toland, J. F. (1992), 'Bifurcation of two curves of T-periodic solutions with zero energy $P = m/n + n/m$, $(m, n) = 1$'. Personal Communication: University of Bath.

van der Meer, J. (1985), *The Hamiltonian Hopf bifurcation (Lecture Notes in Mathematics 1160)*, Springer-Verlag, Berlin.

Wiggins, S. (1988), *Global Bifurcations and Chaos : Analytical Methods*, Springer-Verlag, New York, U.S.A.